17th World Conference on Earthquake Engineering, 17WCEE
Sendai, Japan - September 13th to 18th 2020

CYCLIC LATERAL TESTING AND BACKBONE CURVE DEVELOPMENT OF STEEL BUILT-UP HOLLOW BOX COLUMNS IN HIGH AXIAL LOAD

Chung-Che CHOU(1), Guan-Wei CHEN(2)

(1) Professor, Department of Civil Engineering, National Taiwan University, Taipei, Taiwan, cechou@ntu.edu.tw
Head, Building Engineering Division, National Center for Research on Earthquake Engineering (NCREE), Taipei, Taiwan
(2) Graduate Student Researcher, Department of Civil Engineering, National Taiwan University, Taipei, Taiwan

Abstract

This paper presents testing and backbone curve development of steel high-strength, built-up hollow box columns (HBCs) under combined axial load and cyclic lateral load. Recent studies showed that the seismic performance of steel box columns is strongly influenced by the member compactness, the amount of axial load, and the material yield strength, not concrete infill. Moreover, the width-to-thickness (*b/t*) limit of a highly ductile box column per AISC 341 (2016) is much stringent compared to AIJ (2010) or Taiwan Code (2010). Both the ASCE 41 (2014) and NIST (2017) may also significantly under-estimate the cyclic lateral strength of steel box columns under high axial loads. Therefore, six full-scale, built-up hollow box column specimens, made of high-strength SM 570M steel with the actual yield strength between 460 and 530 MPa, were planned for the experimental program. Three parameters that affect the seismic performance of HBCs were investigated, which includes the *b/t* ratio of the section, the magnitude of axial load, and the lateral loading history (i.e., symmetric *versus* near-fault cyclic displacement histories). The column specimens, which were 290-400 mm in width and 4000 mm in height, were tested with both ends fixed, constant axial loads between 2591 to 7935 kN, and cyclic lateral drifts. The HBC specimens that satisfied the *b/t* requirement of a highly ductile member, as per AISC 341 (2016), under a high axial load (40%P_y) performed satisfactorily at 4% lateral drift and experienced flange and web fractures at 5% lateral drift. However, the HBC specimens that satisfied the most compactness requirement per AIJ (2010) or Taiwan Code (2010), not AISC 341 (2016), did not perform well at 4% drift, losing the axial load carrying capacity due to significant column local buckling and column shortening. Therefore, a less stringent *b/t* requirement leads to poor seismic performance of HBCs under a medium-to-high axial load at 4% drift. The gathered test data, supported by test data of this work, was analyzed by using multiple regression analysis. Empirical relations were derived between the maximum column moment, column plastic rotation and post-yield hardening parameters. The proposed formulation reasonably predicts the first-cycle envelope curves of steel box columns under combined axial load and lateral load, and provides significant improvement of the current ASCE 41 (2014) and NIST (2017) models for steel built-up hollow box columns.

Keywords: Built-Up Hollow Box Column; Cyclic Testing; Local Buckling; Fracture; Backbone Curve Development.

1. Introduction

Steel built-up hollow box columns (HBC) are commonly used in steel structural buildings. The HBC, fabricated by welding four plates together to form a built-up box shape, is similar to a cold-formed steel hollow structural section (HSS) column. Several experiments have been conducted to characterize the hysteretic behavior of HBC or HSS columns under cyclic loading; the studies showed that their seismic performance is strongly influenced by the compactness of steel member, the amount of axial load, and the material yield strength, not concrete infill. However, the AISC-341 [1], AIJ [2] or Taiwan Code [3] have significantly different width-to-thickness (*b/t*) requirements for a highly ductile box member, leading to different column sections in design, particularly in a high seismic area.

To characterize the post-peak strength deterioration of HSS columns, researchers have investigated the seismic performance of HSS columns with different *b/t* and P/P_y ratios, where P is an applied axial compression load and P_y is an axial yield load of the column member [4-6]. Kurata et al. [7] investigated the cyclic behavior of HSS columns under a constant axial load with nominal steel yield strength of 400 MPa. The study showed that the HSS columns with a compact section under a medium axial compressive load of 30%P_y can develop good seismic performance at an interstory drift of 3%. Fadden and McCormick [8] tested 11 steel HSS columns under lateral cyclic drifts without axial load; the test results also indicated that the *b/t* ratio can significantly affect the column ductility. D'Aniello et al. [9] conducted monotonic and cyclic bending tests on H-shaped and HSS columns using the cantilever column setup without axial compression. The test results exhibited strength degradation lower in monotonic loading than in cyclic loading because the local buckling was observed only in a compressed part at the column base. Wang et al. [10] studied the cyclic behavior of welded-box columns with *b/t* ratios of 10 and 20, which satisfy the *b/t* limit per Eurocode 3 [11], the most compact section. The welded box specimens under an axial load of 30%P_y could reach an interstory drift of 3% with minor strength degradation, but did not develop acceptable hysteretic behavior beyond 3% drift. Shi et al. [12] conducted tests on high-strength steel welded box columns with *b/t* ratios of 20-32 and a constant axial load of 20%P_y. The specimens with *b/t* ratios less than 25 could perform well at drifts 2-3%, but the strength degradation was fast and significant after reaching the peak strength.

Suzuki and Lignos [13] studied the effect of lateral loading protocols on the hysteretic behavior of steel HSS columns. Two HSS columns with *b/t* ratios of 26.7 and 19.1 were larger than the *b/t* limit of the highly ductile member per AISC-341 [1], but the latter was considered to be the most compact section, commonly used in high-rise steel construction in Japan. These two specimens under an axial load of 30%P_y developed peak strength at 2% drift and degraded more than 40% of the lateral strength before 4% drift. Chou and Wu [14] investigated the seismic performance of steel hollow box columns (HBCs) and high-strength concrete filled steel box columns, showing that the addition of concrete inside a steel hollow box column under high axial load does not increase the number of cycles to failure. In other words, it is not promising to count on high-strength concrete inside a box column to reduce the *b/t* limit of the steel HBC for sustaining a high axial load at large drifts (i.e.> 3%). Therefore, the objective of this study was to evaluate the effects of the *b/t* limit, axial load, and loading protocols on the seismic performance of high-strength HBCs under a combination of constant axial load and cyclic lateral load. All specimens were tested by double curvature flexural bending after the constant axial compression load was applied, ranging from 2591 kN (582 kips) to 7935 kN (1785 kips).

Although these tests showed that the plastic deformation capacity of steel columns is strongly influenced by the cross-section compactness and the applied axial load, the backbone curves of ASCE 41 [15] and NIST [16] for square columns do not properly describe the post-peak behavior, particularly for large-size columns with *b/t* ratios less than 20 and under large axial loads. The goal of the testing program was to characterize the hysteretic behavior of built-up HBC under various lateral-loading histories coupled with medium-to-high axial compressive load. Researchers [7, 10-13] showed that the HSS column or built-up HBC, designed as the most compact section per AIJ [2] or Eurocode 3 [11] under a medium axial load of 30%P_y, can perform well before a lateral drift of 3%. The seismic performance of these columns under an axial load, exceeding 30%P_y, is not assured at 4% lateral drift. The test data of this work, supported by gathered test data from previous works, is analyzed using multiple regression analysis. Empirical relations are derived for the column maximum moment, plastic rotation and post-yield hardening parameters, and compared to the cyclic test results and the backbone curves of ASCE 41 [15] and NIST [16].

2. Specimen Plan

Fig. 1 shows gathered test data of HBC and HSS members, plotted per the axial load-to-yield load (P/P_y) ratio and the width-to-thickness (b/t) ratio. Three vertical lines are b/t limits for the highly ductile and the most compact built-up box member, which are 12.9, 22, and 21.7 based on AISC 341 [1], AIJ [2] and Taiwan code [3], respectively. The b/t limit of the highly ductile member per AISC 341 [1] is:

$$\lambda_{hd}=0.65\sqrt{E/R_y F_{yn}} \quad (1)$$

where E is the elastic modulus, 200000 MPa, F_{yn} is the nominal yield strength, 420 MPa, for SM570M steel, and R_y is the material over-strength factor, 1.2. The ASIC 341 [1] and AIJ [2] have different b/t limits for built-up compression members, which results in significant thickness difference in design.

Six column specimens were prepared for the work using the high-strength SM570M steel with the actual yield strength between 460 and 530 MPa (Table 1). The test parameters include the b/t ratio, P/P_y ratio, and loading protocol. The specimens are labeled using the column type, b/t ratio, P/P_y ratio, and loading protocol. For example, Specimen HBC-16-40-A is a HBC with a b/t ratio of 16 and is subjected to an axial load of 40%P_y and a loading protocol A, which is a symmetric drift history for testing the beam-to-column moment connection, as specified in AISC 341 [1]. The loading protocols B and C are un-symmetric drift histories, which are near-fault drift protocols developed for steel columns based on Lin et al. [17]. Table 1 shows six square built-up box column specimens with the section ranging from 290 to 400 mm and a clear height of 4000 mm. Both ends of the specimen are fixed to the test facility MATS (Fig. 2) so a double curvature bending test can be conducted after applying the axial compression load, as seen in other works using the MATS facility [14, 18].

All six specimens listed in Table 1 satisfy the most compact section requirement per AIJ [2], Taiwan code [3], and the compact (λ_p=24.4) or moderate ductile (λ_{md}=23.5) sections per AISC 360 [19] and AISC 341 [1], respectively. Specimen HBC-11-40-A that has a b/t ratio of 11 satisfies the requirement of λ_{hd} (=12.9) and is subjected to the same axial load intensity and lateral loading protocol as Specimen HBC-16-40-A that does not meet the highly ductile memebr requirement. Specimens HBC-12-40-B and HBC-12-40-C satisfy the highly ductile member requirement of AISC 341 [1] and are tested with near-fault drift histories [17] with a displacement pulse in an unsymmetric drift protocol, followed by a symmetric drift history (Fig. 3). The objective is to evaluate the post near-fault earthquake strength after the columns experience a near-fault drift protocol.

3. Test Program and Results

Specimen HBC-16-40-A was subjected to a high axial load of 40%P_y and exhibited minor and significant local buckling of the steel box column at 2 and 3% drifts, respectively. The strength degradation started at the first cycle of 4% drift (Fig. 4(a)) due to significant inward buckling of the flange plate near the toe of stiffeners (Fig. 5(a)); the post-peak strength was below 75% of the maximum value in the second cycle. The axial shortening limit of the test setup was reached when the specimen entered the second negative cycle of 4% drift, where the axial load decreased from 3228 to 1120 kN in order to reach the peak displacement of second -4% drift (Fig. 6(a)). Note that when the axial compressive load decreased, the HBC did not show further shortening, indicating that the HBC with a b/t ratio of 16 might perform well at 4% drift with a low axial compressive load (i.e. 1120 kN close to 10%P_y).

Specimens HBC-20-25-A and HBC-14-30-A under a medium axial compression load of 25-30%P_y, instead of 40%P_y, could complete two 4% drift cycles with strength degradation of 5-18% (Fig. 4(b)). Although these two specimens were the compact section, not a highly ductile member per AISC 341 [1], their seismic performance was acceptable at 4% drift with only local buckling near the top and bottom end of the column.

Table 1 Specimen dimension and material properties

Specimen	d (mm)	b=d-2t (mm)	t (mm)	b/t	F_y (MPa)	F_u (MPa)	Axial force (kN)
HBC-16-40-A	290	258	16	16.1	460	586	3228
HBC-20-25-A	360	328	16	20.5	460	586	2591
HBC-14-30-A	400	350	25	14	530	666	6028
HBC-11-40-A	385	329	28	11.8	490	609	7935
HBC-12-40-B	315	271	22	12.3	500	623	5225
HBC-12-40-C	315	271	22	12.3	500	623	5225

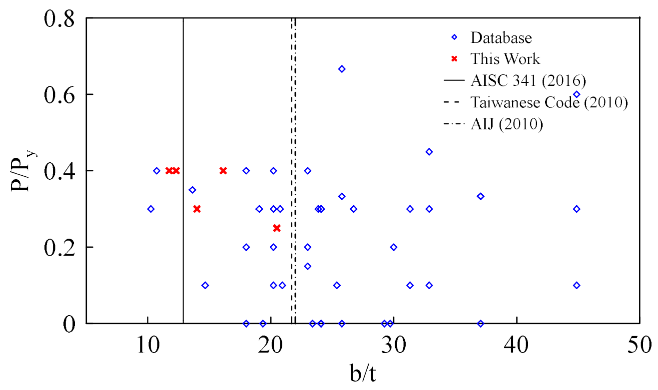

Fig. 1 b/t ratios versus P/P_y ratios

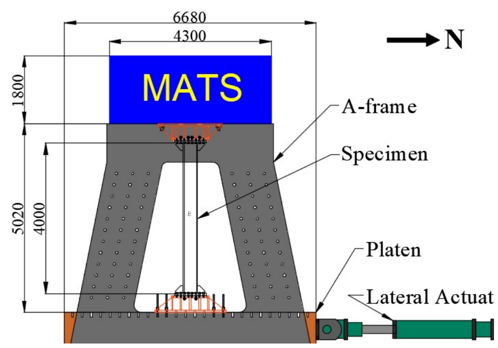

Fig. 2 Test Setup

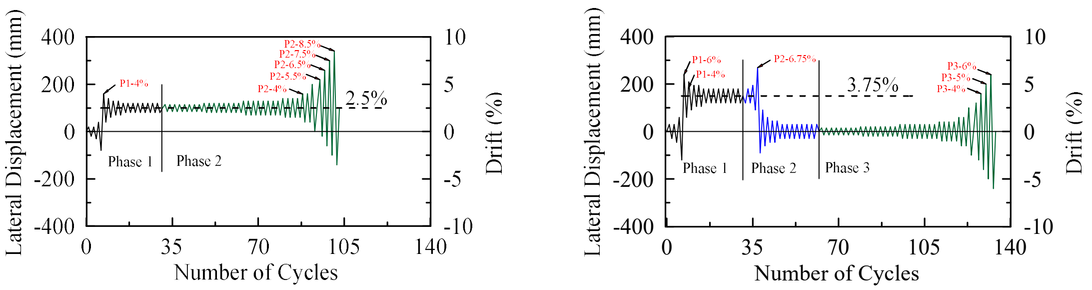

(a) Protocol B

(b) Protocol C

Fig. 3 Near-fault drift histories

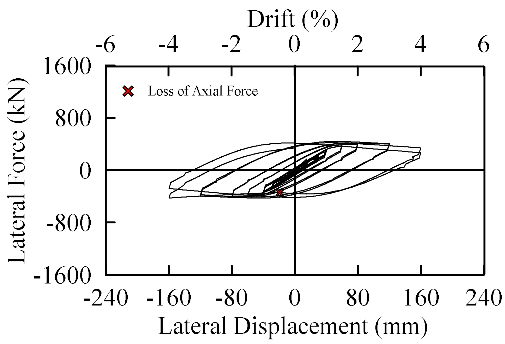

(a) HBC-16-40-A

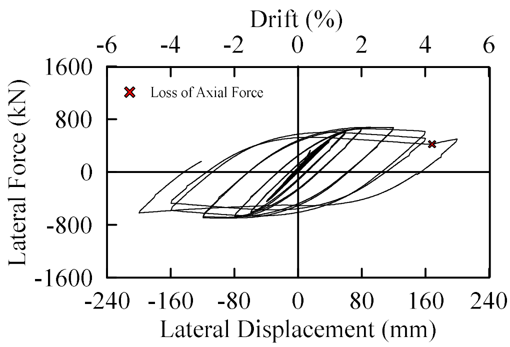

(b) HBC-20-25-A

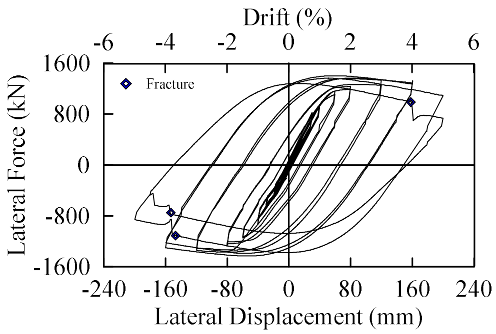

(c) HBC-11-40-A

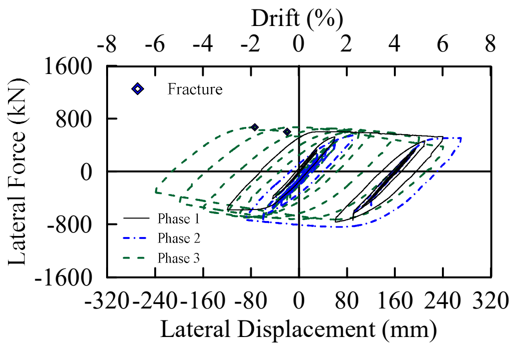

(d) HBC-12-40-C

Fig. 4 Lateral force versus displacement response

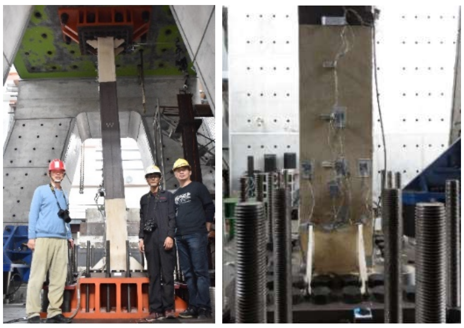
(a) HBC-16-40-A (+4% Drift)

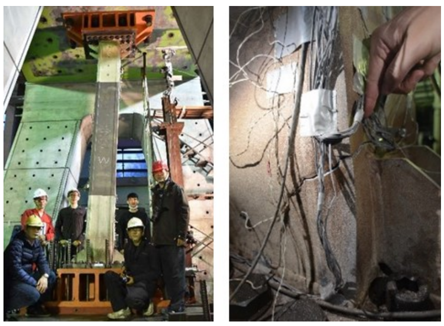
(b) HBC-11-40-A (-5% Drift)

Fig. 5 Observed performance of two specimens

Specimen HBC-11-40-A with a *b/t* ratio less than the limit (=12.9) of a highly ductile member was under a high compression load (=40%P_y) and performed satisfactorily at 4% lateral drift (Fig. 4(c)), exhibiting a similar response as Specimen HBC-14-30-A under a medium axial load of 30%P_y. During the first excursion to -5% drift cycle, the north bottom flange fractured throughout the entire flange (Fig. 5(b)). The second fracture occurred at the top plastic hinge while the specimen was moved in the second excursion of 5% cycle. The third fracture occurred at the top south flange during the second excursion to -5% cycle. Although the flexural strength degraded to 65% of the maximum value at 5% drift (Fig. 4(c)), the axial load carrying capacity did maintain throughout the test with an axial shorting of 108 mm, corresponding to the axial strain of 2.7% (Fig. 6(b)). The test results between Specimens HBC-16-40-A and HBC-11-40-A indicate that as long as the HBC satisfies the *b/t* limit of a highly ductile member per AISC 341 [1], even under a high axial load (40%P_y), it can complete 4% drift cycles with minor strength degradation. However, the most compact section requirement per AIJ code [2] or Taiwan code [3] can assure the HBC to perform well at 3% drift for carrying a high axial load of 40%P_y or at 4% drift for carrying a medium axial compression load, 25-30%P_y.

Specimen HBC-12-40-C under a near-fault displacement protocol performed very well in Phase 1 test up to 6% drift (Fig. 4(d)). Since the displacement history had only one big pulse in the loading direction (Fig. 3(b)), the local buckling was observed in only one column flange in compression without strength degradation in Phase 1 test. The specimen still performed satisfactorily in the post near-fault loading (the symmetric drift history). The strength degradation could be clearly observed in Specimen HBC-12-40-C in Phase 3 test, with significant local buckling on column flanges. The high axial load was maintained throughout three test phases with the axial strain of 2.9%.

4. Development of Cyclic Backbone Curves

The ASCE 41 [15] and NIST [16] specify cyclic backbone curves to model the flexural behavior of columns using four and three zones, respectively. This work adopts the NIST approach, which is also similar to those of Lignos and Krawinkler [20] and Ozkula et al. [21] to model the HBC using three zones. To assess the deterioration of HBCs under varying axial load and cyclic bending, 42 experimental data, which includes tubular hollow structural sections (HSSs) and built-up hollow box sections (HBCs), were collected from past works to conduct the regression analysis. The axial load ratio P/P_y varies from 0 to 0.67, the b/t ratio varies from 10 to 45, and the steel yield strength, F_y, is from 250-530 MPa.

Zone 1

The column specimen in the test includes shear and flexural deformation so that the elastic stiffness, K_e, is estimated based on the flexural stiffness, K_b, and shear stiffness, K_s [16, 21]:

$$K_e = \frac{K_s\, K_b}{(K_s + K_b)} \tag{2}$$

$$K_s = \frac{GA_w\,(KL)}{2};\ K_b = \frac{6EI_x}{KL}(1 - \frac{P}{P_e});\ P_e = \frac{\pi^2 EI_x}{(KL)^2} \tag{3}$$

where K is the effective length factor, I_x is the moment of inertia, P_e is the Euler buckling load, and P is applied axial load. The yield flexural strength, M_y, is calculated based on AISC 341 [1], so the elastic yield rotation, θ_y, is M_y/K_e.

Zones 2 and 3

The pre-buckling plastic rotation, θ_p, and the maximum moment, M_{max}, are needed to define in Zone 2. The strain hardening ratio, α, is defined as the maximum moment, M_{max}, divided by M_y. The rotation corresponding to M_{max} is θ_{max}, and the post-buckling rotation, θ_{pc}, is defined in Zone 3. The calibration process was applied to all 42 gathered data.

Regression Analysis Results

Fig. 7 illustrates the sensitivity of the strain hardening ratio α, pre-buckling plastic rotation, θ_p, and post-buckling rotation, θ_{pc}, to b/t ratio for the data. The coefficient of determination R^2 of linear regression for each parameter versus b/t is low, indicating that the data exhibits some scatter but the trend between these parameters is clear. The parameters α, θ_p, and θ_{pc} strongly depend on b/t ratio and decrease with the increase of b/t ratio.

A function form that was proposed by Lignos and Krawinkler [20] and Ozkula et al. [21] was used in this study to determine the response variables (RV), which are α, θ_p, and θ_{pc}, versus parameters b/t, P/P_y, and F_y. For the cyclic backbone curve, the regression analysis yields the following results:

$$\alpha = (10)^{0.34}\left(\frac{b}{t}\right)^{-0.21}\left(1 - \frac{P}{P_y}\right)^{-0.4} \qquad (R^2 = 0.54) \tag{4}$$

$$\theta_p = (10)^{3.52}\left(\frac{b}{t}\right)^{-1.53}\left(1-\frac{P}{P_y}\right)^{-0.42}(F_y)^{-1.24} \quad (R^2=0.58) \tag{5}$$

$$\theta_{pc} = (10)^{1.06}\left(\frac{b}{t}\right)^{-1.54}\left(1-\frac{P}{P_y}\right)^{2.16}(F_y)^{-0.04} \quad (R^2=0.49) \tag{6}$$

where F_y is the actual yield strength of the column in MPa and a_1 to a_4 are coefficients to be determined from the multivariate regression analysis, which is valid for b/t ($10\leq b/t\leq 45$), P/P_y ($0\leq P/P_y\leq 0.6$), and F_y (250 MPa$\leq F_y\leq$550 MPa).

Fig. 8 shows the compassion between the hysteretic response of specimens and cyclic backbone curves of NIST [16], ASCE 41 [15], and this work (marked by HBC & HSS). In general, the curves proposed by ASCE 41 [15] are significantly conservative compared to those based on NIST [16] and this work. The cyclic backbone curves proposed in this work agree the test response much better than ASCE 41 [1] and NIST [16]. Three predictions are close to the pre-buckling response of Specimen HBC-20-25-A under a medium axial load of 25%P_y (Fig. 8(a)), but show large differences for Specimens HBC-16-40-A or HBC-11-40-A under a high axial load of 40%P_y (Fig. 8(b)). Moreover, the cyclic backbone curves based on ASCE 41 [15] and NIST [16] are overly conservative for estimating the hysteretic response of HBCs under near-fault loading protocols.

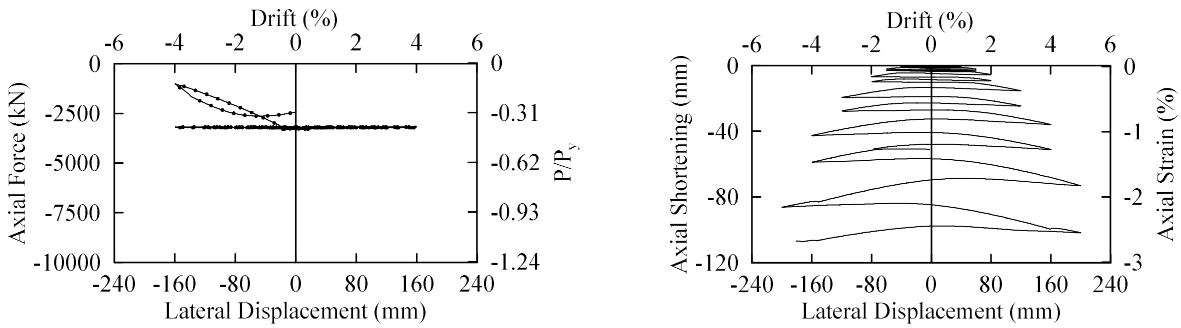

(a) HBC-16-40-A (b) HBC-11-40-A

Fig. 6 Column axial behavior versus lateral displacement

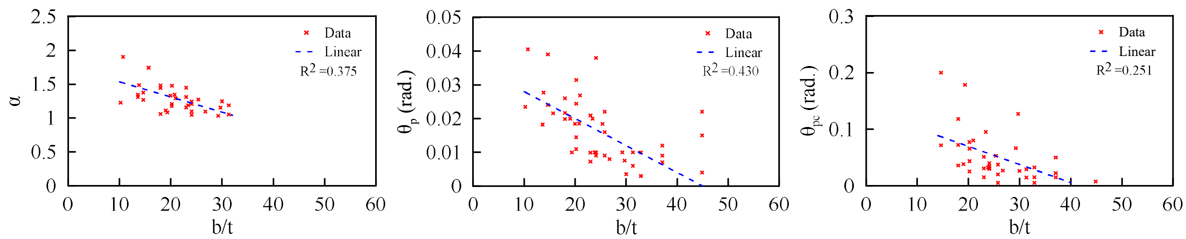

Fig. 7 Data relationship between response variables and *b/t* ratios

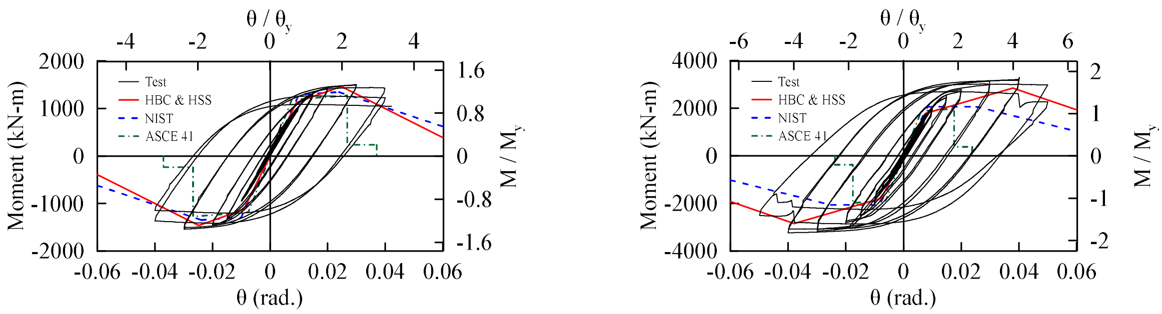

(a) HBC-20-25-A (b) HBC-11-40-A

Fig. 8 Comparison between predictions and test results

5. Conclusions

Six built-up hollow box columns (HBC), made of high-strength SM570 MC steel (actual yield strength 460-530 MPa) with *b/t* ratios between 11 and 20, were tested to investigate their seismic performance. The *b/t* limit of a highly ductile member is 12.9 based on AISC 341 [1]; the most compact *b/t* requirements per AIJ [2] or Taiwan code [3] are 22 and 21.7, respectively. Therefore, all specimens satisfy the most compact requirements per AIJ and Taiwan codes, but only three specimens satisfy the highly ductile requirement per AISC 341 [1]. The objective of the test program was to evaluate the seismic performance of built-up box column specimens under various axial loads and lateral cyclic loads. Cyclic backbone curves that consider the section compactness, axial load and yield strength of columns were proposed based on the test data and additional 36 column specimens under cyclic loading (Fig. 1).

For Specimens HBC-11-40-A and HBC-16-40-A under a high axial load (40%P_y), Specimen HBC-11-40-A, with a *b/t* ratio of 11, completed 4% drift cycles and then exhibited fracture of buckled plates at 5% drift. Specimen HBC-16-40-A, with a *b/t* ratio of 16, completed 3% drift cycles and degraded below 90% of the peak strength in the first cycle of 4% drift. Although Specimen HBC-20-25-A with a larger *b/t* ratio and under a lower axial load intensity than Specimen HBC-16-40-A, Specimen HBC-20-25-A degraded below 72% of the peak strength in the second cycle of 4% drift. Therefore, limiting a *b/t* ratio below the limit of a highly ductile member based on AISC 341 [1] postpones local buckling of steel plates and assures good seismic performance of HBCs under a high axial load (=40%P_y) at 4% drift cycles (Fig. 4(c) and Fig. 5(b)). However, the built-up box column designed by following the most compact *b/t* limit of AIJ [2] or Taiwan code [3] can assure good seismic performance at 3 or 4% drifts under medium axial loads (25-30%P_y), which may be classfied as a moderate ductile member (Fig. 4(a) and (b)). Cyclic backbone curves were proposed based on the gathered column test data of built-up hollow box sections and hollow structural sections under symmetric loadings. The proposed backbone curves that consider the strain hardening and plastic rotation in accordance with the variation of *b/t*, P/P_y and F_y reasonably predict the first cycle response of the specimens in this work. Three predictions are close to the pre-buckling response of Specimen HBC-20-25-A under a medium axial load of 25%Py (Fig. 8(a)), but the predictions based on ASCE 41 [15] and NIST [16] are too conservative for column specimens under a high axial load (Fig. 8(b)). A US-Taiwan collaborative research work has been conducted through two-story steel subassembages to study boundary condition of column ends on the column behavior [22].

Acknowledgements

This study was supported by the Ministry of Science and Technology (Grant No. MOST 107-2625-M-002-013). The test was conducted at the National Center for Research on Earthquake Engineering (NCREE), Taiwan. The assistance from the technician is gratefully acknowledged.

References

[1] ANSI, AISC 341-16. (2016). *Seismic provisions for structural steel buildings,* 60601.

[2] AIJ (2010). *Recommendation for limit state design of steel structures*. Architectural Institute of Japan.

[3] Taiwan Code (2010). *Design and technique specifications of steel structures for buildings*. Construction and Planning Agency Ministry of the Interior, Taiwan.

[4] Kouichi Y., Yamada. S. (1984). Elasto plastics deformation and fracture behavior of steel box columns subjected to double curvature cyclic bending under constant axial load. *Proceedings of AIJ*.

[5] Tsuda and Matsui, C. (1998). Strength of square steel tubular beam-columns under constant vertical and horizontal loads. *J. Structural Construction Engineering*, AIJ, 512, 149-156.

[6] Uenoya, M., Nakamura, M., Fukumoto, Y., & Yamamoto, S. (2002). An experimental study on the elastic-plastic hysteretic behavior of tapered box columns. *International Journal of Steel Construction Engineering*, 9(33), 25-35 (in Japanese).

[7] Kurata, M., Nakashima, M., & Suita, K. (2005). Effect of column base behaviour on the seismic response of steel

moment frames. *J. Earthquake Engineering*, 9, 415-438.

[8] Fadden, M., McCormick, J. (2011). Cyclic quasi-static testing of hollow structural section beam members. *J. Structural Engineering*, ASCE, 138(5), 561-570.

[9] D'Aniello, M., Landolfo, R., Piluso, V., & Rizzano, G. (2012). Ultimate behavior of steel beams under non-uniform bending. *J. Constructional Steel Research*, 78, 144-158.

[10] Wang, Y. B., Li, G. Q., Cui, W., & Chen, S. W. (2014). Seismic behavior of high strength steel welded beam-column members. *J. Constructional Steel Research*, 102, 245-255.

[11] CEN, Eurocode 3, 2005, *Design of steel structures, part 1-1, general rules and rules for buildings*, EN 1993-1-1, Brussels: European Committee for Standardization.

[12] Shi, G., Wang, J.J., Bai, Y., & Shi, Y. (2014). Experimental study on seismic behavior of 460MPa high strength steel box-section columns. *Advances in Structural Engineering*, 17(7), 1045-1059.

[13] Suzuki, Y., Lignos, D. (2017). Collapse behavior of steel columns as part of steel frame buildings: experiments and numerical models. *16th World Conference on Earthquake Engineering*. International Association of Earthquake Engineering.

[14] Chou, C. C., Wu, S. C. (2019). Cyclic lateral load test and finite element analysis of high-strength concrete-filled steel box columns under high axial compression. *Engineering Structures*, 189, 89-99.

[15] ASCE. 2014. *Seismic evaluation and retrofit of existing buildings*, ASCE 41-13. American Society of Civil Engineers, Virginia, USA.

[16] ATC. 2017. *Guidelines for Nonlinear Structural Analysis for Design of Buildings*: Part IIa – Steel Moment Frames, NIST GCR 17-917-46v2.

[17] Lin T. H., Chou, C. C., & Chen, G. W. (2019). A seven-story steel braced frame under far-field and near-fault earthquakes: loading protocol and seismic test of high-strength steel H-shaped columns. *International Conference in Commemoration of 20th Anniversary of the 1999 Chi-Chi Earthquake.* Taiwan. Sep. 15-19.

[18] Chou, C. C., Lee, C. S., Wu, K. Y., & Chin, V. L. (2018). Development and validation of a FRP-wrapped spiral corrugated tube for seismic performance of circular concrete columns. *Construction and Building Materials*, 170, 498-511.

[19] ANSI, B. AISC 360-16, *Specification for Structural Steel Buildings*. Chicago, IL: American Institute of Steel Construction, 2016.

[20] Lignos, D.G., Krawinkler, H., 2010, "A steel database for component deterioration of tubular hollow square steel columns under varying axial load for collapse assessment of steel structures under earthquakes," *7th International Conference on Urban Earthquake Engineering (7CUEE) & 5th International Conference on Earthquake Engineering (5ICEE)*, Tokyo Institute of Technology, Tokyo, Japan.

[21] Ozkula, G., Harris, J., & Uang, C. M. (2017). Cyclic backbone curves for steel wide-flange columns: A numerical study. *EUROSTEEL*, Copenhagen, Denmark, 3365-3374.

[22] Chou, C. C., Lin, T. H., Xiong, H. C., Lai, Y. C., Uang, C. M., El-Tawil, S., McCormick, J. P., Mosqueda G. (2019). US-Taiwan collaborative research on steel columns: cyclic testing of two-story subassemblages. *International Conference in Commemoration of 20th Anniversary of the 1999 Chi-Chi Earthquake.* Taiwan. Sep. 15-19.

